

DESY 04-045

March 2004

A new technique to generate 100 GW-level attosecond X-ray pulses from the X-ray SASE FELs

E.L. Saldin, E.A. Schneidmiller, and M.V. Yurkov

Deutsches Elektronen-Synchrotron (DESY), Notkestrasse 85, Hamburg, Germany

Abstract

We propose a scheme for generation of single 100 GW 300-as pulse in the X-ray free electron laser with the use of a few cycles optical pulse from Ti:sapphire laser system. Femtosecond optical pulse interacts with the electron beam in the two-period undulator resonant to 800 nm wavelength and produces energy modulation within a slice of the electron bunch. Following the energy modulator the electron beam enters the first part of the baseline gap-adjustable X-ray undulator and produces SASE radiation with 100 MW-level power. Due to energy modulation the frequency is correlated to the longitudinal position within the few-cycle-driven slice of the SASE radiation pulse. The largest frequency offset corresponds to a single-spike pulse in the time domain which is confined to one half-oscillation period near the central peak electron energy. After the first undulator the electron beam is guided through a magnetic delay which we use to position the X-ray spike with the largest frequency offset at the "fresh" part of the electron bunch. After the chicane the electron beam and the radiation produced in the first undulator enter the second undulator which is resonant with the offset frequency. In the second undulator the seed radiation at reference frequency plays no role, and only a single (300 as duration) spike grows rapidly. The final part of the undulator is a tapered section allowing to achieve maximum output power 100-150 GW in 0.15 nm wavelength range. Attosecond X-ray pulse is naturally synchronized with its fs optical pulse which reveals unique perspective for pump-probe experiments with sub-femtosecond resolution.

1 Introduction

Time-resolved experiments are used to monitor time-dependent phenomena. The study of dynamics in physical systems often requires time resolution beyond the femtosecond capabilities. Subfemtosecond capabilities are now available in the XUV wavelength range [1,2]. This is achieved by focusing a fs laser into a gas target creating radiation of high harmonics of fundamental laser frequency. In principle, table-top ultra-fast X-ray sources have the right duration to provide us with a view of subatomic transformation processes. However, their power and photon energy are by far low. There also exists a wide interest in the extension of attosecond techniques into the 0.1 nm wavelength range.

With the realization of the fourth-generation light sources operating in the X-ray regime [3,4], new attoscience experiments will become possible. In its initial configuration the XFEL pulse duration is about 100 fs, which is too long to be sufficient for this class of experiments. The generation of subfemtosecond X-ray pulses is critical to exploring the ultrafast science at the XFELs. The advent of attosecond X-ray pulses will open a new field of time-resolved studies with unprecedented resolution. X-ray SASE FEL holds a great promise as a source of radiation for generating high power, single attosecond pulses. Recently a scheme to achieve pulse duration down to attosecond time scale at the wavelengths around 0.1 nm has been proposed [5]. It has been shown that by using X-ray SASE FEL combined with terawatt-level, sub-10-fs Ti:sapphire laser system it will be possible to produce GW-level X-ray pulses that are reaching 300 attoseconds in duration. In this scheme an ultrashort laser pulse is used to modulate the energy of electrons within the femtosecond slice of the electron bunch at laser frequency. Energy-position correlation in the electron pulse results in spectrum-position correlation in the SASE radiation pulse. Selection of ultra-short X-ray pulses is achieved by using the monochromator. Such a scheme for production of single attosecond X-ray pulses would offer the possibility for pump-probe experiments, since it provides a precise, known and tunable interval between the laser and X-ray sources.

In this paper we propose a new method allowing to increase output power of attosecond X-ray pulses by two orders of magnitude. It is based on application of sub-10-fs laser for slice energy modulation of the electron beam, and application "fresh bunch" techniques for selection of single attosecond pulses with 100 GW-level output power. The combination of very high peak power (100 GW) and very short pulse (300 as) will open a vast new range of applications. In particular, we propose visible pump/X-ray probe technique that would allow time resolution down to subfemtosecond capabilities. Proposed technique allows to produce intense ultrashort X-ray pulses directly from the XFEL, and with tight synchronization to the sample excitation laser. Another advantage of the proposed scheme is the possibility to remove the monochromator (and other X-ray optical elements) between the X-ray undulator and a sample and thus to directly use the probe attosecond X-ray pulse.

2 High power attosecond facility description

A basic scheme of the high-power attosecond X-ray source is shown in Fig. 1. An ultra-short laser pulse is used to modulate the energy of electrons within the femtosecond slice of the electron bunch at laser frequency. The seed laser pulse will be timed to overlap with the central area of the electron bunch. It serves as a seed for modulator which consists of a short (a few periods) undulator. Following the energy modulator the beam enters the baseline (gap-tunable) X-ray undulator. In its simplest configuration the X-ray undulator consists of an uniform input undulator and nonuniform (tapered) output undulator separated by a magnetic chicane (delay). The process of amplification of radiation in the input undulator develops in the same way as in conventional X-ray SASE FEL: fluctuations of the electron beam current serve as the input signal [6]. When an electron beam traverses an undulator, it emits radiation at the resonance wavelength $\lambda = \lambda_w(1 + K^2/2)/(2\gamma^2)$. Here λ_w is the undulator period, $mc^2\gamma$ is the electron beam energy, and K is the undulator parameter. In the proposed scheme the laser-driven sinusoidal energy chirp produces a correlated frequency chirp of the resonant radiation $\delta\omega/\omega \simeq 2\delta\gamma/\gamma$.

Our concept of attosecond X-ray facility is based on the use of a few cycle optical pulse from Ti:sapphire laser system. This optical pulse is used for modulation of the energy of the electrons within a slice of the electron bunch at a wavelength of 800 nm. Due to extreme temporal confinement, moderate optical pulse energies of the order of a few mJ can result in electron energy modulation amplitude higher than 30-40 MeV. In few-cycle laser fields high intensities can be "switched on" nonadiabatically within a few optical periods. As a result, a central peak electron energy modulation is larger than other peaks. This relative energy difference is used for selection of SASE radiation pulses with a single spike in time domain. Single-spike selection can effectively be achieved when electron bunch passes through a magnetic delay and output undulator operating at a shifted frequency. A schematic, illustrating these processes, is shown in Figs. 2 and 3.

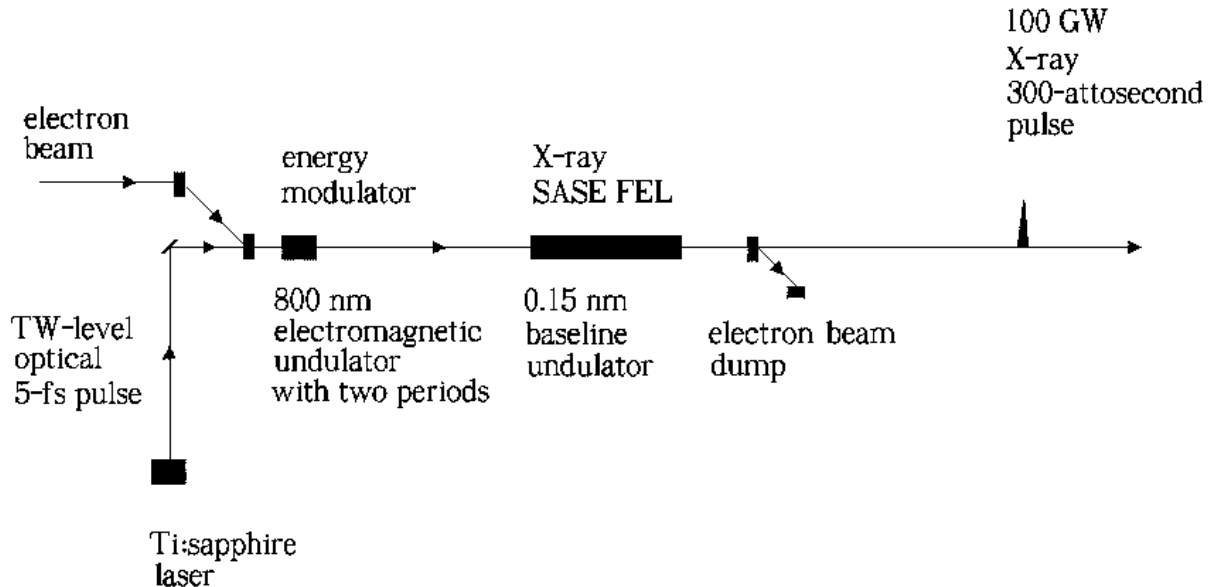


Fig. 1. Schematic diagram of high power attosecond X-ray source

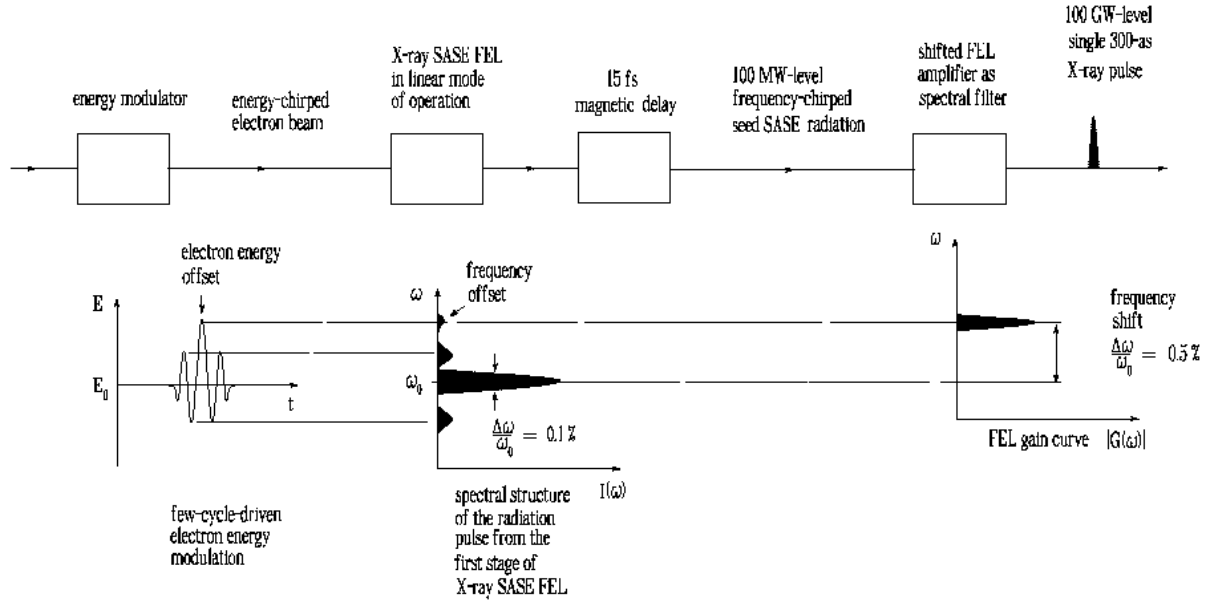


Fig. 2. Sketch of high power attosecond X-ray pulse synthesis through frequency chirping and spectral filtering

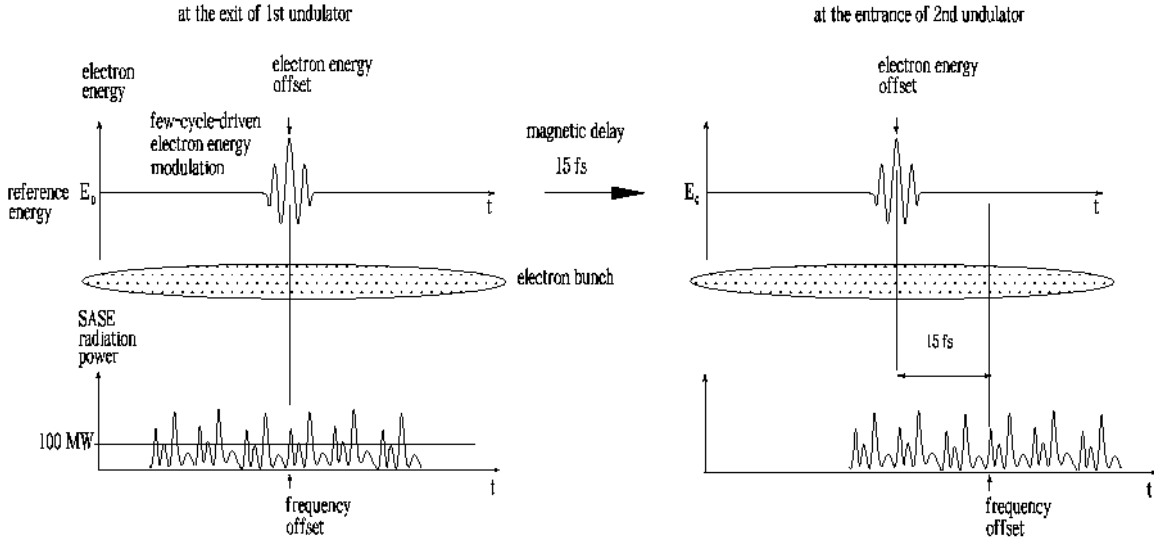


Fig. 3. Sketch of principle of "fresh bunch" technique

The input undulator is a conventional 0.15 nm SASE FEL operating in the high-gain linear regime. This undulator is long enough (60 m) to reach 100 MW-level output power (see Fig. 4). After the input undulator the electron beam is guided through a magnetic delay (chicane). The trajectory of the electron beam in the chicane has the shape of an isosceles triangle with the base equal to L . The angle adjacent to the base, θ , is considered to be small. Parameters in our case are: $L = 4$ m, $\theta = 1.5$ mrad, compaction factor $L\theta^2 = 8\mu\text{m}$, extra path length $L\theta^2/2 = 4\mu\text{m}$, horizontal offset $L\theta/2 = 3$ mm. In the present design we have only $4\mu\text{m}$ extra path length for the electron beam, while the FWHM length of electron bunch is about $50\mu\text{m}$. Calculations of the coherent synchrotron radiation effects show that this should not be a serious limitation in our case.

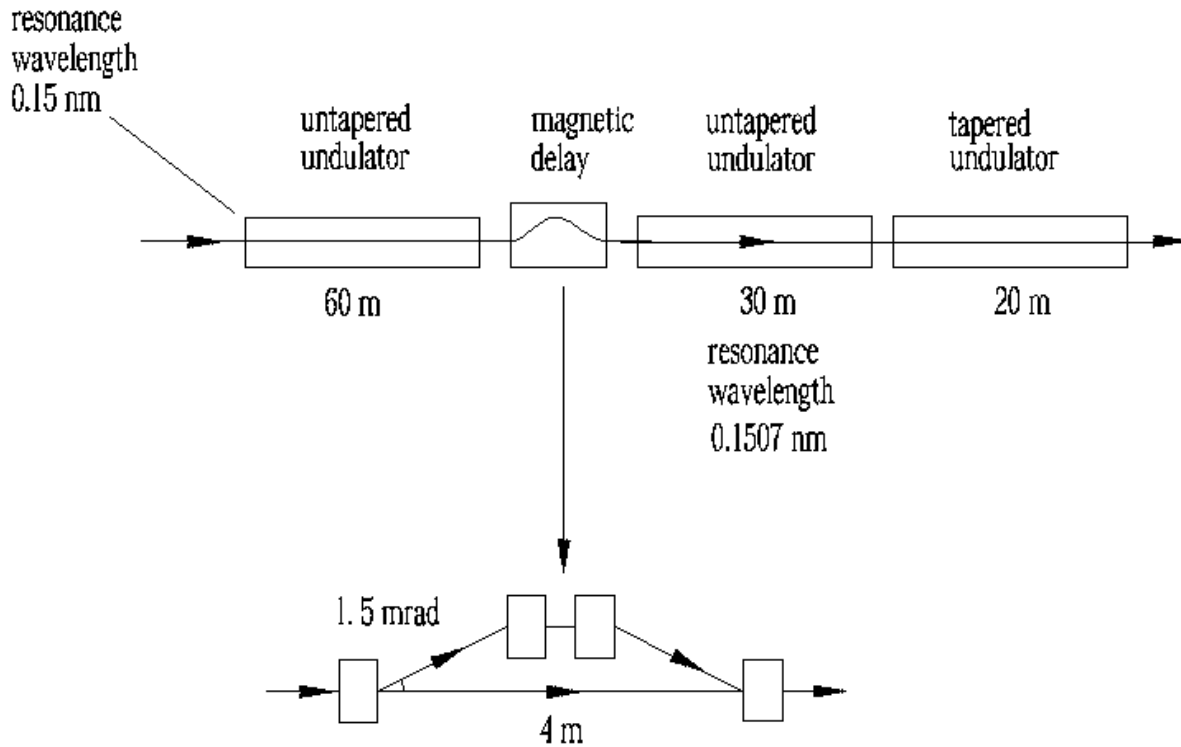


Fig. 4. Design of undulator system for high power attosecond X-ray source

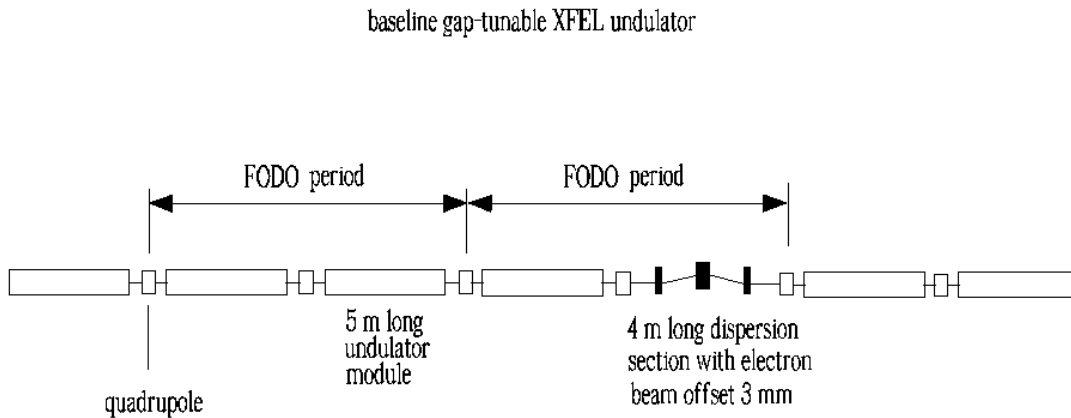


Fig. 5. Installation of a magnetic delay in the baseline XFEL undulator. The quadrupole separation of a FODO lattice is large enough so that magnetic chicane of length 4 m can be installed

Passing the chicane the electron beam and seed SASE radiation enter the output undulator operating at an offset frequency. We use a magnetic delay to position the offset frequency radiation at the "fresh" part of the electron bunch. This seed single spike at an offset frequency starts interacting with the new set of electrons, which have no energy modulation, since they did not participate in the previous interaction with optical laser pulse (see Fig. 3). This is the essence of the "fresh bunch" techniques which was introduced in [7].

In the output undulator seed radiation at reference frequency plays no role. However, single spike at an offset frequency is exponentially amplified upon passing through the

baseline gap-tunable XFEL undulator modes of operation

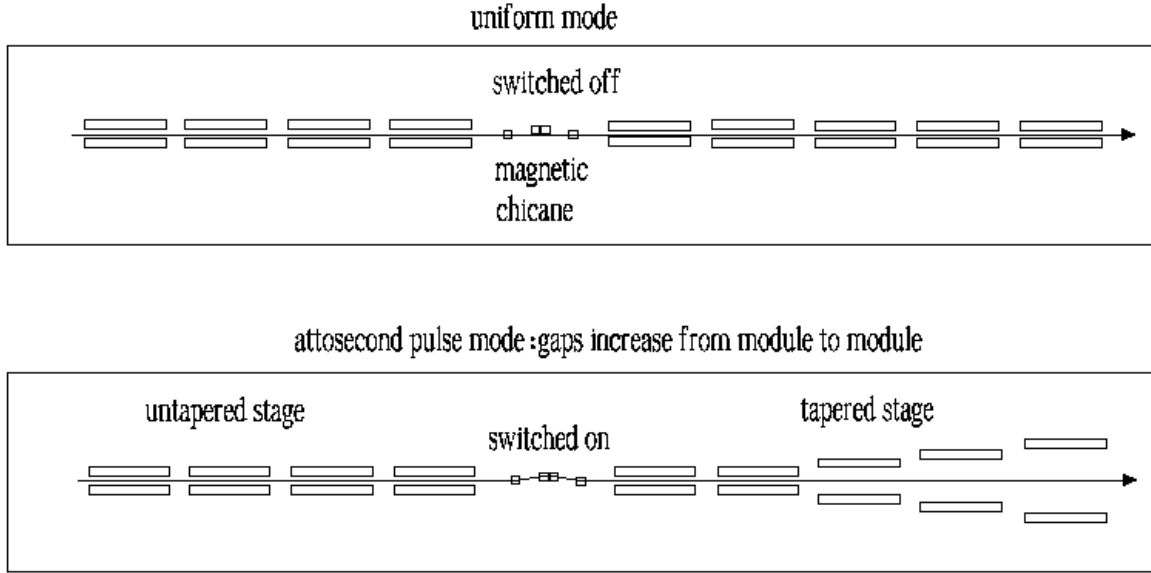


Fig. 6. Baseline XFEL undulator allowing different modes of operation for SASE FEL. Tuning of the radiation wavelength and magnetic field tapering is provided by changing the gap

first (uniform) part of the output undulator. This part is long enough (30 m) to reach saturation. The power level at saturation is about 20 GW. The most promising way to extend output power is the method of tapering the magnetic field of the undulator. Tapering consists in slowly reducing the field strength of the undulator field to preserve the resonance wavelength as the kinetic energy of the electrons changes. The strong radiation field produces a ponderomotive well which is deep enough to trap the particles. The radiation produced by these captured particles increases the depth of the ponderomotive well, and they are effectively decelerated. As a result, much higher power can be achieved than for the case of a uniform undulator. At the total tapered undulator length of 20 m, the single-spike power is enhanced by a factor of five, from 20 GW-level to 100 GW-level. With the baseline gap-tunable undulator design this option would require only installation of a magnetic delay. The quadrupole separation of an undulator FODO lattice (5 m) is large enough so that relatively short (4 m) magnetic chicane can be installed (see Fig. 5). The undulator taper could be simply implemented as a step taper from one undulator segment to the next. Figure 6 shows the design principle of undulator for attosecond mode of operation.

Our study shows that the method proposed in this paper allows direct production from XFEL of single 100 GW-level X-ray pulses with FWHM duration of 300 as. Contrast of a single spike is mainly defined by the amplification of shot noise in the main part of electron bunch. This effect leads to degradation of contrast of output attosecond X-ray pulses. However, parameters of the undulator system can be optimized in such a way that the contrast degradation is insignificant. Calculation shows that in optimum case the ratio of the attosecond pulse power (signal) and SASE pulse power (background) at the undulator exit reaches a value of 400.

3 Generation of 100 GW-level attosecond pulses from XFEL

Operation of 100 GW attosecond SASE FEL is illustrated for the parameters close to those of the European XFEL operating at the wavelength 0.15 nm [3]. Optimization of the attosecond SASE FEL has been performed with the three-dimensional, time dependent code FAST [8] taking into account all physical effects influencing the SASE FEL operation (diffraction effects, energy spread, emittance, slippage effect, etc.). The parameters of the electron beam are: energy 15 GeV, charge 1 nC, rms pulse length 25 μm , rms normalized emittance 1.4 mm-mrad, rms energy spread 1 MeV. Undulator period is 3.65 cm.

The parameters of the seed laser are: wavelength 800 nm, energy in the laser pulse 2–4 mJ, and FWHM pulse duration 5 fs (see Fig. 7). The laser beam is focused onto the electron beam in a short undulator resonant at the optical wavelength of 800 nm. Optimal conditions of the focusing correspond to the positioning of the laser beam waist in the center of the modulator undulator. It is assumed that the phase of laser field corresponds to "cosine" mode (solid line with $\varphi = 0$, see Fig. 7). Parameters of the modulator undulator are: period length 50 cm, peak field 1.6 T, number of periods 2. The interaction with the laser light in the undulator produces a time dependent electron energy modulation as it is shown in Fig. 7. For the laser (FWHM) pulse duration of 5 fs at a laser pulse energy 2-4 mJ, we expect a central peak energy modulation of 30-40 MeV.

SASE undulator consists of three sections. First section is 57 meter long uniform undulator. Second section is 28 meters long uniform undulator with different resonance frequency. Frequency detuning between the second and the first undulator section is $\Delta\omega/\omega = 0.6\%$. The third section is 20 meters long tapered undulator. A dispersion section with 8 μm net compaction factor is placed between the first and the second undulator sections.

Figure 8 shows evolution of energy in the radiation pulse along the undulator. Generation of powerful attosecond X-ray pulses is performed in three-step procedure. Electron beam enters the first undulator section. Amplification process develops from the shot noise in the electron beam. Figure 9 shows temporal structure of the radiation pulse in the end

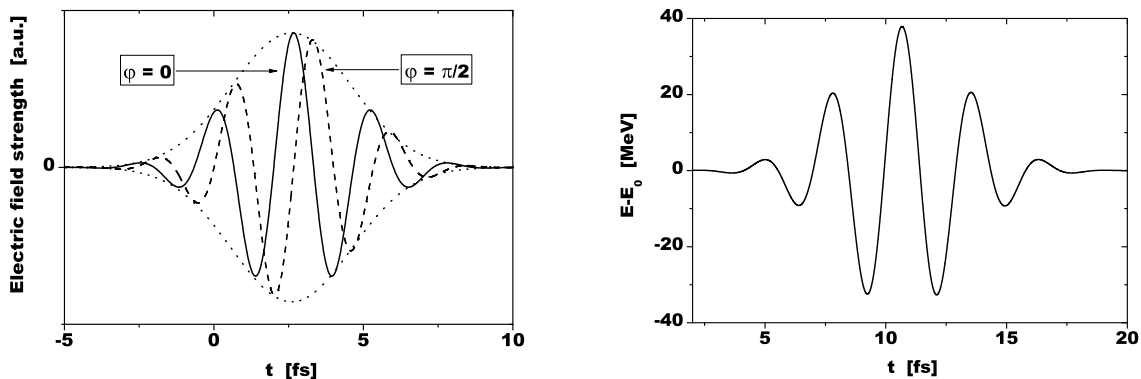


Fig. 7. Left plot: electric field strength within femtosecond laser pulse. Right plot: energy modulation of electron bunch at the exit of the modulator

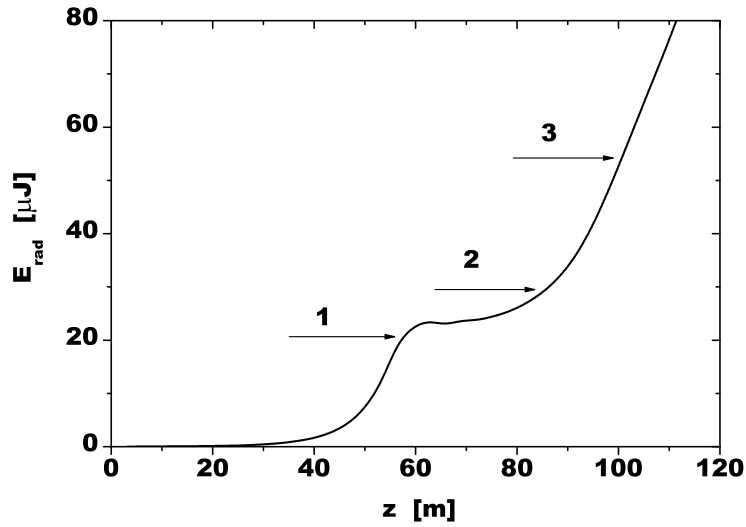


Fig. 8. Energy in the radiation pulse versus undulator length. Marks 1, 2, and 3 show the end points of the 1st, 2nd, and 3rd undulator sections, respectively

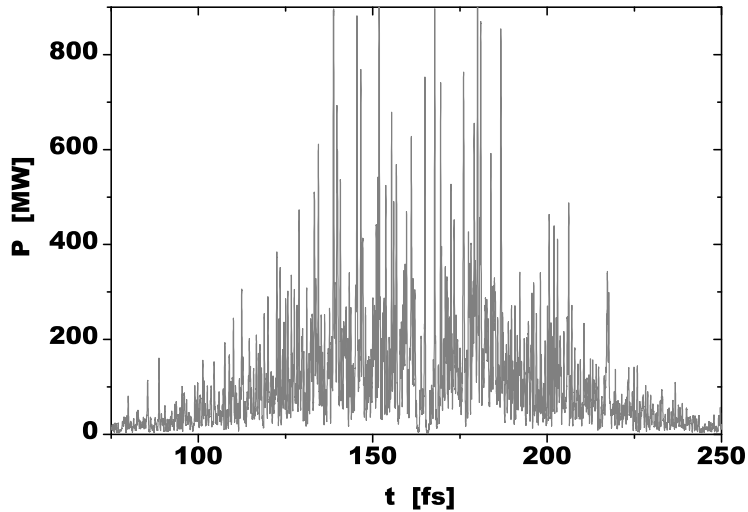


Fig. 9. Temporal structure of the radiation pulse in the end of the first undulator section

of the first undulator section. Top plots in Fig. 10 show enlarged view of temporal structure and spectral structure. A signature of the slice beam modulation is clearly seen in the temporal structure of the radiation pulse. The dotted line in this figure shows the initial energy modulation of the electron beam. The temporal structure of the radiation pulse has a clear physical explanation. The FEL process is strongly suppressed in the regions of the electron bunch with large energy chirp, and only regions of the electron bunch with nearly zero energy chirp produce radiation. From a physical point of view each part of the bunch near the local extremum of the energy modulation can be considered as an isolated

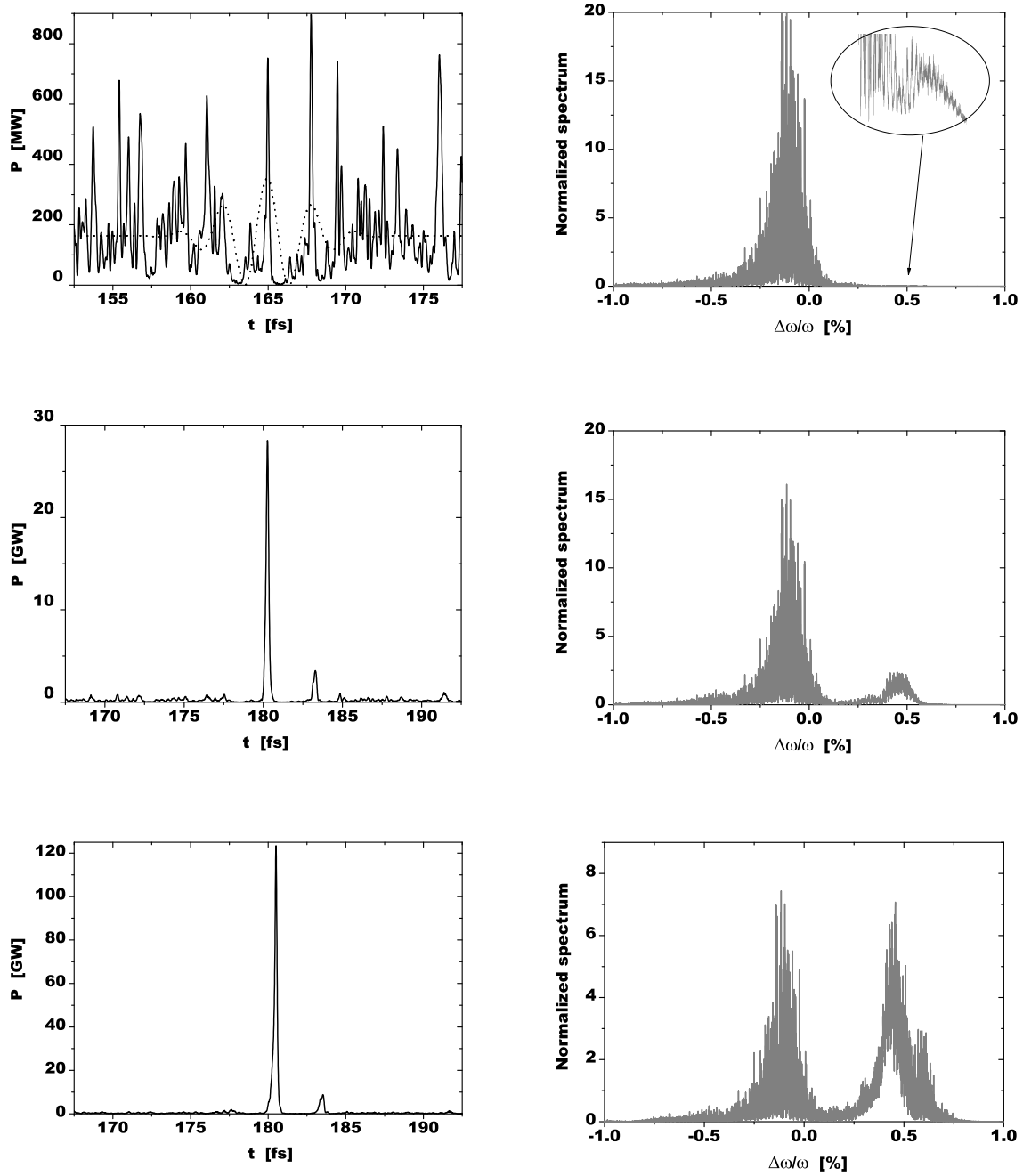


Fig. 10. Temporal (left column) and spectral (right column) evolution of the radiation pulse along the undulator. Upper, middle, and lower plots correspond to the undulator lengths of 57, 85, and 100 m. Dashed line shows energy modulation of the electron bunch

electron bunch of short duration. At the chosen parameters of the system its duration is about 300 attosecond which is about of coherence time. Thus, it is not surprising that only a single radiation spike is produced by each area near the local extremum. Note that each of these spikes (wavepackets) has significant frequency offset from the frequency of the main radiation pulse. For instance, frequency detuning of the spike corresponding to time $t = 165$ fs is about 0.5%. It is hardly noticeable on the scale of complete spectrum

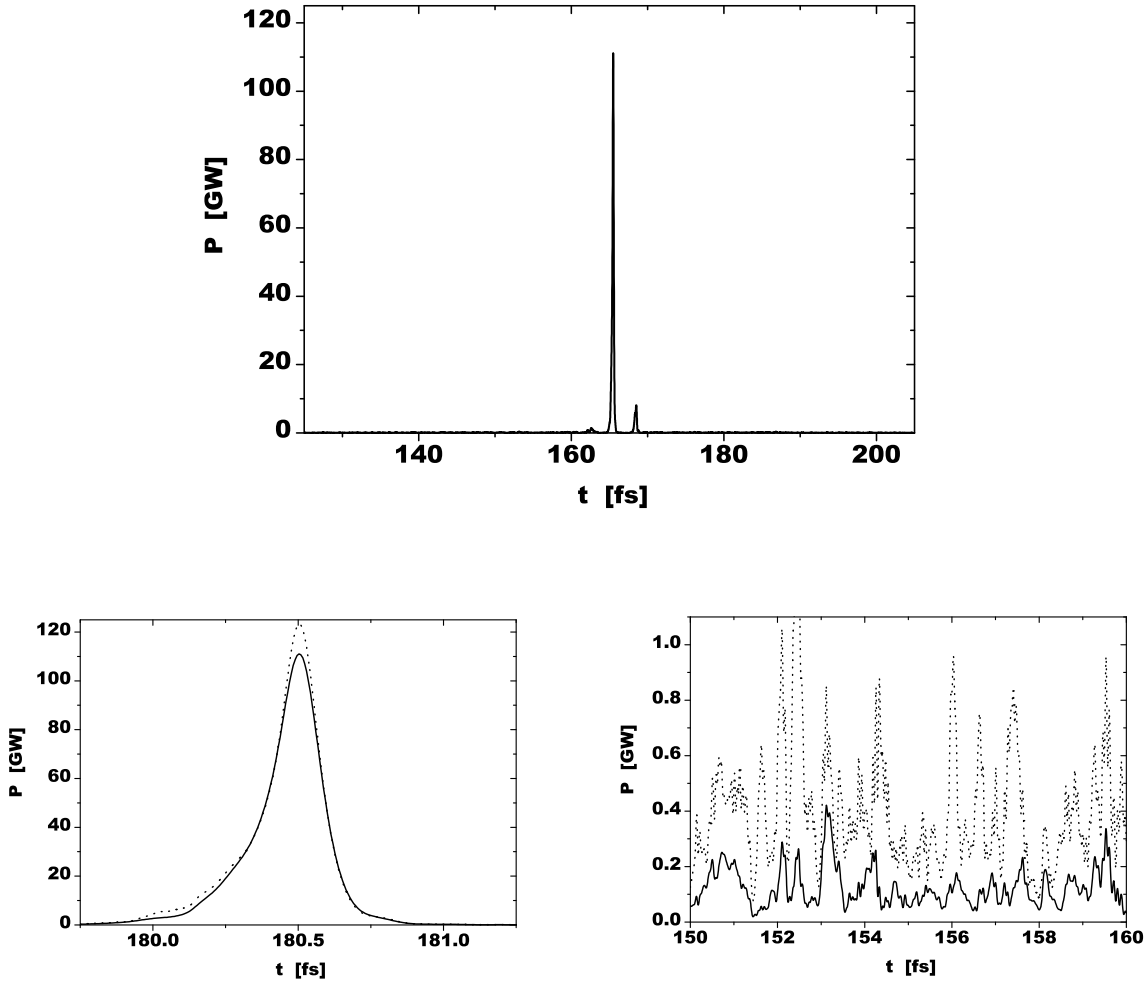


Fig. 11. Temporal structure of the radiation pulse after monochromator with 0.5% linewidth tuned to the frequency of the main maximum. Undulator length is 100 m. Plots at bottom show enlarged view of the top plot. Dotted lines show temporal profile of the radiation pulse before monochromator

of the radiation pulse, since its contribution to the total radiation energy is a fraction of a per cent.

At the next step the electron beam passes the dispersion section. The dispersion section performs two actions. First, it provides delay of the electron bunch by 15 fs with respect to the radiation pulse, such that the radiation produced by modulated slice of the electron bunch slips forward to "fresh", nonmodulated part of the bunch. Second, the strength of dispersion section is sufficient for suppression of the beam bunching. As a result, the amplification process in the second undulator section starts with "fresh" electron beam and radiation seed produced by the first undulator section. The undulator of the second section is tuned to $\Delta\omega/\omega = 0.6\%$ in order to provide the resonance with the radiation produced by the slice of the electron bunch having maximum energy offset. Under such conditions only a single spike is amplified effectively as it is illustrated with

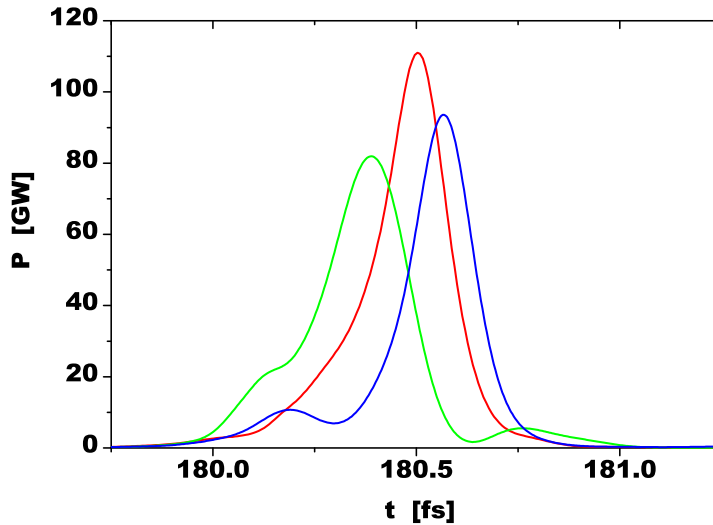


Fig. 12. Shot-to-shot fluctuations of the radiation pulse after monochromator with 0.5% linewidth tuned to the frequency of the main maximum. Undulator length is 100 m

plots in Fig. 10. The rest part of the seed radiation pulse has significant detuning and propagates without visible interaction with the electron bunch. Amplitude of a single attosecond pulse grows exponentially with the undulator length, and enters to saturation regime with peak power of about 20 GW. In order to increase peak power to 100 GW level final (the third) undulator section is tapered. Bottom plots in Fig. 10 illustrate typical temporal and spectral structure of the radiation pulse at the exit of the SASE undulator. In principle, much higher than 100 GW peak power in the attosecond pulse can be achieved. However, one should keep in mind the background produced by the rest of the electron bunch. The seed radiation from the first undulator section is not a problem, it has large frequency offset and can be simply filtered by multilayer monochromator. The main limiting factor is the growth of the radiation from the shot noise which has the same frequency spectrum as attosecond pulse. When attosecond pulse enters nonlinear stage of amplification, noise background still continues to grow exponentially, and can reach high power. This effect imposes a limit on the allowable undulator length (and on peak power of the attosecond pulse). Figure 11 shows temporal characteristics of the radiation pulse at the exit of the undulator (dotted lines). Solid lines in this plot show properties of the radiation pulse after monochromator with 0.5% linewidth. It is seen that the contrast of the radiation pulse is pretty high. Figure 12 illustrates shot-to-shot fluctuations of the radiation pulse.

4 Pump-probe experiments with attosecond SASE FEL

The proposed high power, ultra-fast X-ray source holds a great promise as a source of X-ray radiation for such applications as pump-probe experiments. The time resolution of pump-probe experiment is obviously determined by the duration of the pump as well as

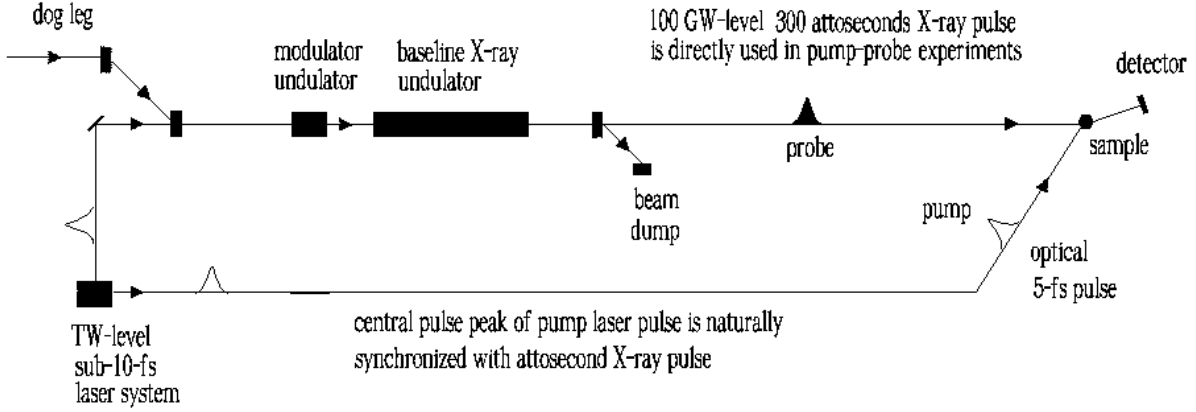


Fig. 13. Scheme for femtosecond resolution pump-probe experiments based on the generation of the 100 GW-level attosecond X-ray pulses directly from X-ray SASE FEL

the resolution of the probing. The pump pulse must always be as short as the desired time resolution. In typical scheme of a pump-probe experiment the short probe pulse follows the pump pulse at some specified delay. The signal recorded by the slow detector then reflects the state of the sample during the brief probing. The experiment must be repeated many times with different delays in order to reconstruct the dynamical process.

We suggest to combine attosecond X-ray pulses with fs optical pulses generated in the seed Ti:sapphire laser system (see Fig. 13) for pump-probe experiments. In this case attosecond X-ray pulse is naturally synchronized with its fs optical pulse, and time jitter is cancelled. Another advantage of the proposed scheme is the possibility to remove all X-ray optical elements between the X-ray source and a sample and thus to directly use the probe attosecond X-ray pulse. Usual optical elements are used for seed laser beam splitting and tunable delay. It should be possible to achieve a timing accuracy close to duration of the half period of the seed laser pulse (1 fs), allowing an unprecedented insight into the dynamics of electronic excitations, chemical reactions, and phase transitions of matter, from atoms, through organic and inorganic molecules, to surface, solids and plasma.

Let us discuss in more detail an attosecond pulse contrast in the proposed scheme for pump-probe experiments based on the use the direct X-ray beam. We wish to consider one example which shows the relationship between the signal and background that is easy to understand. We choose for emphasis here experiments aimed at measuring the lifetime of electronic excitation. First, the time dependence of electronic occupation is assumed to be known – this is an exponential dependence $n(t) = n_0 \exp(-t/\tau_0)$. The typical lifetime of electronic excitation is in the femtosecond range. A time-resolved experiment inherently begins with initiation of the process under study (electronic excitation) at some more or less accurately defined instant in time. The number of photocounts detected during attosecond pulse (probe) is directly proportional to the physical parameter (electronic occupation number) to be measured: $K = AI_a\tau_a n(\tau)$, where I_a is the intensity of attosecond pulse, τ_a is the attosecond pulse duration, and τ is the delay between pump and probe pulses. On the other hand, the number of background photocounts is proportional to the integrated value of the physical parameter: $K = A \int_0^{\infty} I_b(t) n_0 \exp(-t/\tau_0) dt$, where $I_b(t)$ is instantaneous background intensity of SASE radiation. At time $t = 0$ the pump pulse

perturbs the sample. As a result, the average number of background photocounts is about $\langle K \rangle \simeq A \langle I_b \rangle \tau_0 n_0$. The ratio of attosecond intensity and background intensity is about $I_a/I_b \simeq 400$. On the other hand, the ratio of attosecond pulse duration and characteristic time of (sub-10-fs) physical process is about $\tau_a/\tau_0 \simeq 0.1$ only. Thus, we find that effects of SASE background radiation are not important in experiments for the study of the dynamics of the sub-10-fs processes.

It is obvious that proposed pump-probe techniques could be applied at longer time-scale, too. In particular, there exists a wide interest in the extension of light-triggered time-resolved studies to the sub-100-fs timescale. Now we return to the question about an attosecond pulse contrast. According to our discussion above, the number of background photocounts in this case is proportional to integral over the whole SASE radiation pulse with duration of about 300 times longer than the attosecond pulse. Calculation shows that in this case the ratio of attosecond pulse energy to SASE radiation pulse energy reaches a value of about 1:1. The number of photocounts as a function of delay time has thus a peak to background of 2 to 1. These sub-100-fs studies we can refer as time-resolved experiments with the background, as opposed to the background-free time-resolved experiments for study of the sub-10-fs processes. It should be noted that the final time resolution of pump-probe experiments with the background is not worse than that of background-free experiments with the same pump and probe pulse duration, but we secure this resolution with a much higher number of independent measurements.

A scheme of pump-probe experiments for the study of the dynamics of the sub-100-fs processes can be modified to increase significantly the contrast of output attosecond X-ray pulses. A reliable method to decrease the background might be to use a broadband monochromator. One can align the monochromator so that the peak of the SASE radiation spectrum at reference frequency is blocked. To reach the required value of monochromatization is not a problem. For 0.15 nm wavelength range, Bragg diffraction is the main tool used for such purposes. In this case, one has to care that the short pulse duration is preserved. We are discussing here only multilayer X-ray mirrors, which have the largest relative bandwidth [9–11]. Layered synthetic materials – multilayers – are layered structures with usually two alternating materials: a low and high density materials. They play an important role in synchrotron X-ray optics. Typical multilayers used as optical elements at the third generation synchrotrons provide a spectral bandwidth of 0.5 to 5%. Typical glancing angles are of the order of a degree. As a rule, from 100 to 400 periods participate in effective reflection in such mirrors. About 90% peak reflectivity was achieved for wavelengths around 0.1 nm. Analysis presented in this paper shows that this technique has a potential to increase single-spike contrast (ratio of attosecond pulse power to background power) up to 2000. This means that in the proposed scheme of pump-probe experiments with multilayer monochromator the effects of SASE background radiation are not important even in the 100 fs time range.

5 Conclusion

Today there are at least two possible attosecond X-ray sources for light-triggered, time-resolved experiments associated with the X-ray SASE FEL: the "attosecond X-ray

parasitic” [5] and the ”attosecond X-ray dedicated” source mode proposed in this paper. The simplest way to obtain attosecond X-ray pulses from XFEL is to use ”parasitic” technique which is proposed in [5]. It also would offer the possibility of providing a beam to a pump-probe experiments with the XFEL that has a precise, known and tunable time interval between the laser and X-ray sources. More power of attosecond pulse could be obtained using the XFEL for dedicated attosecond X-ray pulse production as described in this paper.

Both types of attosecond X-ray sources are important, their roles are complementary, and one type can not replace the other. The baseline gap-tunable XFEL undulator offers simplicity and flexibility. Different operational modes can be realized with the undulator control system. The baseline XFEL operates in uniform (maximum gain) mode. With no constraints on baseline FEL operation, technique for production of attosecond X-ray pulses which is proposed in [5] could be used. If dedicated attosecond beamtime will be available, an undulator could be tapered (and magnetic chicane could be switched on) to provide more power in attosecond pulses.

Acknowledgments

We thank R. Brinkmann, G. Grübel, J.R. Schneider, A. Schwarz, and D. Trines for interest in this work.

References

- [1] P. Paul, *Science* 292(2001)1689.
- [2] M. Hentchel et al., *Nature* 414(2001)509.
- [3] P. Audebert et al., “TESLA XFEL: First stage of the X-ray laser laboratory – Technical design report (R. Brinkmann et al., Eds.)”, Preprint DESY 2002-167.
- [4] The LCLS Design Study Group, LCLS Design Study Report, SLAC reports SLAC- R521, Stanford, 1998.
- [5] E.L. Saldin, E.A. Schneidmiller and M.V. Yurkov, Preprint DESY 04-013, 2004. Submitted to *Optics Communications*.
- [6] E. L. Saldin, E. A. Schneidmiller and M. V. Yurkov, *The Physics of Free Electron Lasers* (Springer-Verlag, Berlin) 1999.
- [7] L. H. Yu and I. Ben-Zvi, *Nucl. Instrum. and Methods* A393(1997)96.
- [8] E. L. Saldin, E. A. Schneidmiller and M. V. Yurkov, *Nucl. Instrum. and Methods* **A 429**(1999)233.
- [9] P. Deschamps et al., *J. Synchrotron Rad.* 2(1995)124.
- [10] D. Windt, *Appl. Phys. Lett.* 74(1999)2890.
- [11] Ch. Morawe et al., *SPIE Proc.* 4145(2000)61.

